



Cu(II)-Metallacryptands Self-Assembled to Vesicular Aggregates Capable of Encapsulating and Transporting an Anticancer Drug Inside Cancer Cells

Protap Biswas, Koushik Sarkar, and Parthasarathi Dastidar*

Crystallographically characterized M_2L_4 type cationic Cu(II)-metallacryptands [MC(X)] derived from a series of bis-pyridyl-bis-urea ligands (L_X ; X = O, S, C) are self-assembled to single-layered vesicular aggregates in DMSO, DMSO/water, and DMSO/DMEM (biological media). One such vesicle is MC(O)-vesicle that is demonstrated to be able to load and release (pH responsive) an anticancer drug, namely doxorubicin hydrochloride (DOX). DOX-loaded MC(O)-vesicle is also successfully transported within MDA-MB-231 cells—a highly aggressive human breast cancer cell line. Such self-assembling behavior to form vesicular aggregates by metallacryptands (MCs) is hitherto unknown.

“blackberry” type vesicular structure.^[18–21] Studies revealed that counterion-mediated attractions controlled by charge regulation mechanism^[22] is responsible for such spontaneous self-assembly of the cationic MOPs to form such vesicular aggregates. In fact, neutral Cu(II)-MOPs derived from tricarboxylate ligand failed to form vesicles under similar conditions.^[23] It is, therefore, logical to envisage that cationic metallacryptands which are also cage-like entities akin to MOPs might self-assemble to form vesicles. Although there have been a few reports of organic cryptands^[24] being able to form vesicles,^[25,26] cationic metal-

laccryptands displaying such self-assembling ability is hitherto unknown to the best of our knowledge.

1. Introduction

The successful development of membrane in biological system by nature is vital to the existence of life because living cell would not exist without membrane. It holds the content of cell in a confined environment, allows important nutrients to diffuse and help extricate the waste through channels, protects against chemical and biological attacks, and helps in cell division, fertilization, and many more. The building blocks of cell membrane are phospholipids that self-assemble to form bilayer lamellar structure driven by hydrophobic interactions. Inspired by such intriguing structure and functions of cell membrane, scientists have taken keen interests in developing synthetic membrane.^[1] The first totally synthetic molecule capable of self-assembling to form bilayer membrane system, namely lamellae and vesicle, is an organic compound, namely didodecyltrimethylammonium bromide.^[2] Since then, a large number of organic molecules capable of forming vesicles have been reported.^[3–11] However, metal–organic compounds capable of forming such hierarchical structures are limited.^[12–15] Metal–organic-based vesicles have recently been reported for drug delivery applications.^[16,17] Interestingly, metal–organic polyhedra (MOP) have been shown to form single layered

2. Results and Discussion

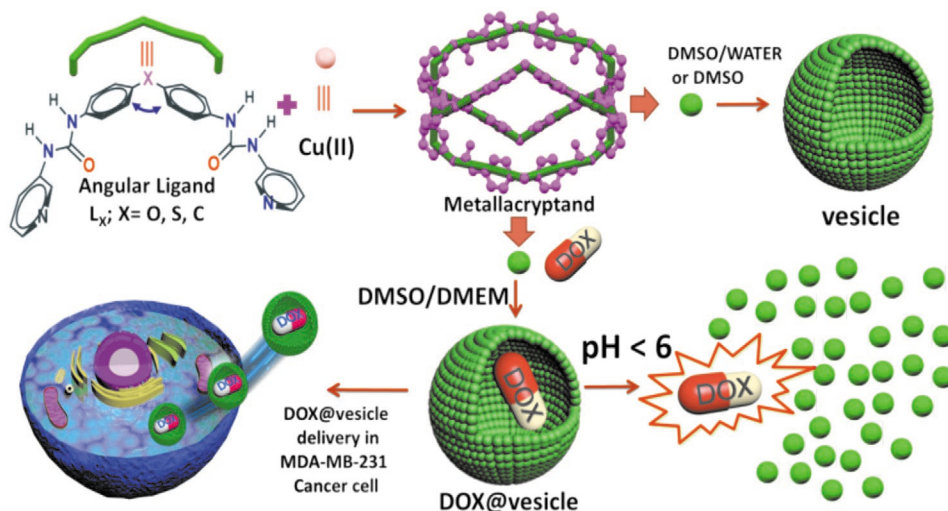
Herein, we report functional vesicles derived from crystallographically characterized metallacryptands (general formulae $\{[Cu_2(L_X)_4 \cdot 2EtOH] \cdot (SiF_6)_2 \cdot nH_2O\}$) obtained by reacting a series of bis-pyridyl-bis-urea ligands (L_X ; X = O, S, C) with in situ generated $CuSiF_6$ (generated from equimolar mixture of $Cu(BF_4)_2$ and $(NH_4)_2SiF_6$ in water). The metallacryptands, thus synthesized, self-assembled to form vesicles in a variety of solvent systems [DMSO, DMSO/ H_2O , and DMSO/biological media, i.e., DMEM], were able to encapsulate and release an anticancer drug doxorubicin hydrochloride (DOX) in vitro in a pH responsive manner. DOX-loaded vesicles could also be transported into a highly aggressive human breast cancer cell line, namely MDA-MB-231 (Scheme 1). Bis-pyridyl-bis-urea ligands (L_X) having varying central atom (X = O, S, C) were chosen because L_X can adopt a bent ligating geometry (due to central $\angle C-X-C \approx 105^\circ$ – 116° and free rotation of the terminal pyridyl rings) conducive for metallacryptand formation.

Our previous studies indicated that metal ion preferring octahedral coordination geometry (e.g., Cu(II)) and counter anion (e.g., SiF_6^{2-}) played a crucial role in synthesizing metallacryptands.^[27] Thus, reaction of L_X (X = O, S, C) and $CuSiF_6$ in DMF/EtOH/water (4:9:2) under layering condition at room temperature afforded single crystals of the metallacryptands namely MC(O), MC(S), and MC(C), respectively, confirmed by single crystal X-ray diffraction (SXRD) studies (Scheme S1 and Table S4, Supporting Information).

P. Biswas, Dr. K. Sarkar, Prof. P. Dastidar
School of Chemical Sciences
Indian Association for the Cultivation of Science (IACS)
2A and 2B, Raja S. C. Mullick Road, Jadavpur, Kolkata,
West Bengal 700032, India
E-mail: ocpd@iacs.res.in

The ORCID identification number(s) for the author(s) of this article can be found under <https://doi.org/10.1002/mabi.202000044>.

DOI: 10.1002/mabi.202000044



Scheme 1. Functional vesicles derived from metallacryptands.

All the metallacryptands were crystallized in the tetragonal space group ($I4/m$) with near identical cell dimensions implying that they were isomorphous. The metal center displayed slightly distorted square pyramidal geometry wherein the equatorial sites were coordinated by the terminal pyridyl moieties of L_x and the axial site was occupied by EtOH through Cu–O coordination; the counter anion SiF₆²⁻ was found to be located outside the cryptand cage. While MC(S) and MC(C) did have lattice occluded water molecules located outside the cryptand cage, MC(O) was devoid of any lattice occluded solvent as per the SXRD data obtained. The approximate size of the metallacryptand cages is $\approx 1.8 \times 1.9$ nm (Figure 1).

The crystalline phase purity of the metallacryptands was found to be reasonably satisfactory as per powder X-ray diffraction (PXRD) patterns (see Figures S23–25, Supporting Information). To see if the cationic metallacryptands, thus synthesized, would self-assemble to form vesicles as envisaged, we carried the following experiments under ambient conditions at room temperature; a highly diluted solution (200 μ M) of the metallacryptands in DMSO was drop-casted on a carbon-coated TEM grid (300 mesh), dried overnight in a vacuum desiccator. Cluster of collapsed spherical objects having average size of ≈ 120 , ≈ 121 , and ≈ 144 nm for MC(O), MC(S), and MC(C), respectively, in the corresponding TEM images was observed. Thus, the collapsed spherical objects which were ≈ 60 – 70 times larger than the MCs (considering average dimension of ≈ 2 nm as per SXRD data) must be the self-assembled hierarchical aggregates

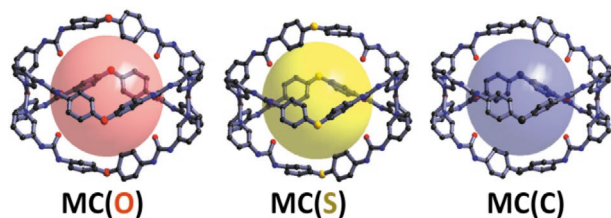


Figure 1. Single crystal structures of metallacryptands (counterions, hydrogen atoms, and the lattice occluded solvents are not shown for clarity).

of the MCs. A burst vesicular structure apparently arising due to solvent evaporation during TEM sample preparation was also evident in the case of MC(O). The thickness of the burst vesicle was found to be ≈ 8 nm. Similar morphology was also observed in the corresponding AFM images; the fact that the spherical objects were collapsed hollow spheres was evident from the much reduced height (5–8 nm) compared to the diameters (≈ 110 nm) of the objects in the images (Figure 2).

Time dependent dynamic light scattering (DLS) data accumulated over a period of 60 days from a DMSO solution (200 μ M) of MC(O) revealed that the hydrodynamic diameter (D_h) of the particles present in such solution was 255 ± 30 nm and the number (%) intensity slowly increased with a narrower size distribution (Figure 3); this may be due to fission and fusion of hollow sphere like particles. The fact that the average D_h was centered around 255 ± 30 nm and remained nearly unchanged over a period of 60 days clearly indicates that the supramolecular assemblies of MC(O) do have preferred curvatures in solution. If the scattering particles were solid nanosphere arising due to close packing of the molecular MCs, there would be 1061208 molecules of MC(O) to fill in the volume of a particle having $D_h = 255$ nm.

On the other hand, in case of hollow sphere having a membrane made of single layered assembly of MC(O), only 41616 molecules of MC(O) are required to cover the surface area of the said particle considering 2.5 nm molecular dimension of MC(O) as per its single crystal structure by taking into account of the van der Waals radii of the atoms (see Figure S26, Supporting Information). Thus, number (%) intensity in DLS would have been much stronger from the very beginning if it were a solid nanosphere. Moreover, the DLS data were similar to that observed for single layered “blackberry” vesicular structures formed by macro-anions like polyoxometalates (POMs)^[28–31] as well as cationic MOPs.^[18–21] It may be noted that the thickness of wall of the burst vesicle was ≈ 8 nm which was 4 times thicker than the diameter of a single MC(O) cage (Figure 2) as evident from its single crystal structure. The reason for such thicker wall as compared to a single layered vesicle is expected in a burst vesicle because of the overlap of

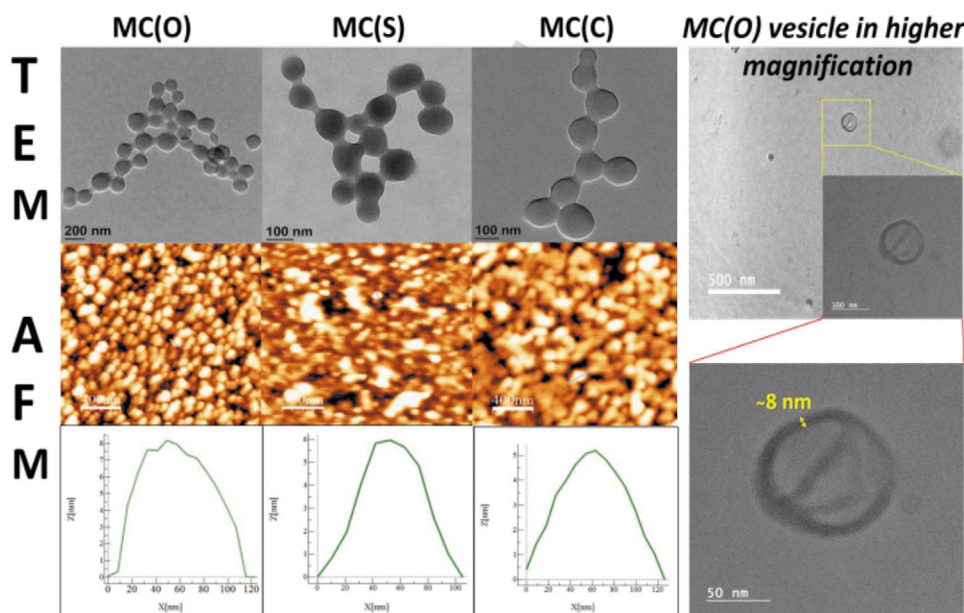


Figure 2. TEM and AFM images (with height profile); scale bar for AFM 400, 300, and 400 nm, respectively (from left to right).

the aggregated MC(O)s arising from top and bottom peripheral surface of the hollow vesicle when collapsed.

The vesicular aggregates of MC(O) and MC(C) were stable up to 100×10^{-6} and 50×10^{-6} M concentration, respectively whereas that of MC(S) started to disintegrate into smaller assemblies at 100×10^{-6} M as evident from DLS measurement as a function of concentration of the MCs. However, we could not see the evidence of molecular MCs under much diluted condition (0.5×10^{-6} M and beyond) (see Figures S27–S29, Supporting Information). The foregoing discussions clearly established that all the MCs produced single layered vesicular architecture in DMSO.

To provide further support to the formation of vesicular architecture, we undertook dye encapsulation studies. For this purpose, dilute solutions of the MCs in DMSO/water (2:98, v/v) in presence of a dye namely calcein were subjected to dialysis.

The bulk solvent was discarded and replenished with fresh load of solvent till no characteristic peak for calcein was detected in UV–vis spectroscopy. Interestingly, characteristic peak of free calcein due to π - π^* transition was found to be redshifted by 13–23 nm in the MC/calcein solution present in the dialysis bag. This data suggested confined environment of the dye arising because of encapsulation within the vesicles formed by the MCs; confined environment of calcein was also evident from the fluorescence quenching compared to free calcein observed in MC/calcein solution obtained after dialysis. Calcein encapsulated vesicles derived from MC(O) could also be seen under a fluorescence microscope (Figure 4). The efficiency of calcein encapsulation was $\approx 15\%$ in all the cases (see Figure S30, Supporting Information). Thus, it is clearly established that the cationic MCs akin to cationic MOPs do form single layered vesicles.

Since organic assemblies are popular target as drug delivery vehicles,^[22–36] we explored the possibility of using metal–organic derived vesicle for that purpose and considered loading a drug in the vesicle derived from MC(O). Thus, an anticancer drug namely doxorubicin hydrochloride (DOX) was encapsulated in MC(O)-vesicle by following similar protocol of calcein encapsulation (see above). As expected, the λ_{\max} of MC(O)/DOX experienced redshift by 17 nm in the UV–vis spectra and its fluorescence intensity was significantly quenched compared to that of free DOX indicating encapsulation of DOX within the vesicle. Interestingly, DOX encapsulated vesicle could easily be seen under a fluorescence microscope (Figure 5).

The encapsulation efficiency of DOX in MC(O)-vesicle was found to be $\approx 4\%$ (see Supporting Information). DLS data accumulated from MC(O) solution (200×10^{-6} M in DMSO) as a function of pH clearly indicated the disruption of the vesicular structure to smaller aggregates; particles having $D_h \approx 50$ nm were observed at pH 4 (Figure 6a) suggesting that the encapsulated DOX could be released in a stimuli responsive manner

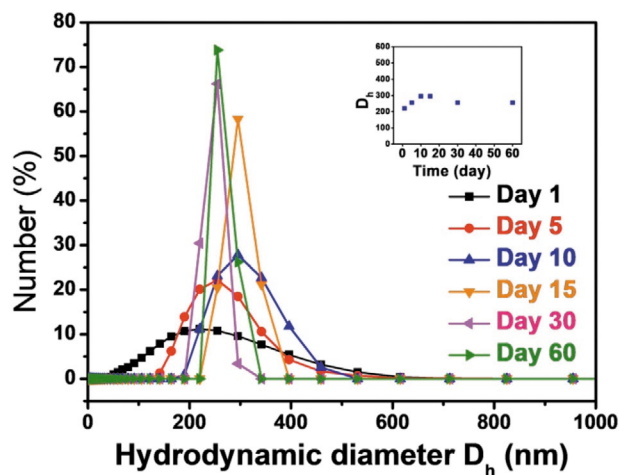


Figure 3. Time dependent DLS data of MC(O)-vesicle.

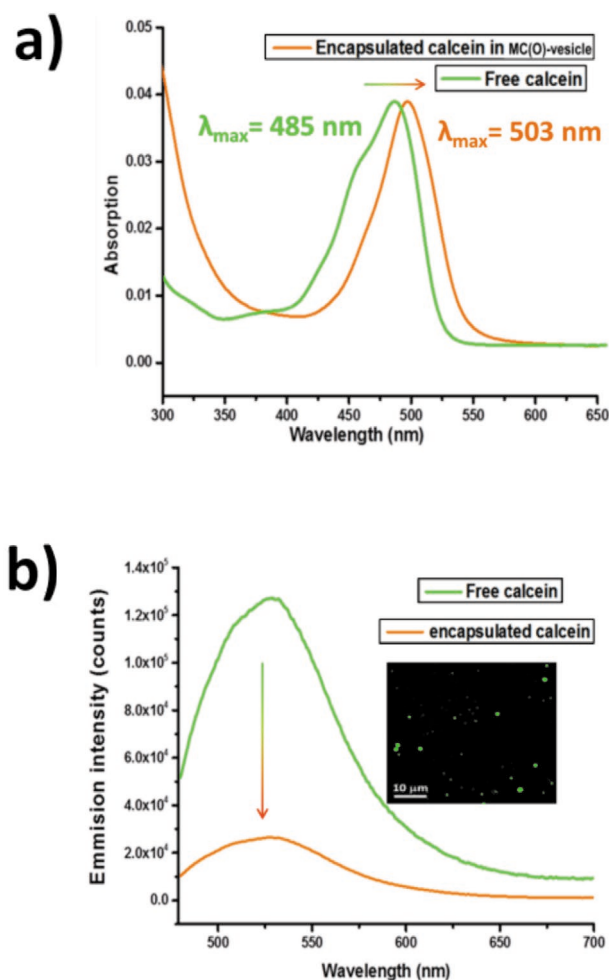


Figure 4. a) UV-vis and b) emission spectra of calcein under different conditions (inset: fluorescence microscope image of calcein encapsulated MC(O) vesicles).

(see Experimental Section). In fact, pH dependent emission spectra of DOX@MC(O)-vesicle showed gradual increase in fluorescence intensity (Figure 6b) of DOX suggesting disruption of the vesicles and delivery of DOX into the bulk solvent. Time dependent DOX release from DOX@MC(O)-vesicle at a select pH 5 showed that near completion release of the drug required 12 h (Figure S38, Supporting Information). Such pH responsive drug release could be quite useful in killing cancer cells since pH of cancer cells is found to be often acidic.^[37,38] Concentration dependent DLS data (see Figure S27, Supporting Information) established that the observed degradation of the vesicular aggregate was not due to dilution effect. It may be mentioned that the vesicles studied here are made from cationic metallacryptands having SiF_6^{2-} as counter anion. Therefore, under lower pH (acidic pH), the counter anions as well as the other proton accepting functionalities (e.g., urea moiety and ethereal O atom of the ligand) are expected to get protonated thereby disrupting assembly structure. Moreover, at a significantly lower pH (pH 2), demetalation of the metallacryptand is also a possibility resulting in total degradation of the ligand as well as the assembly structure.

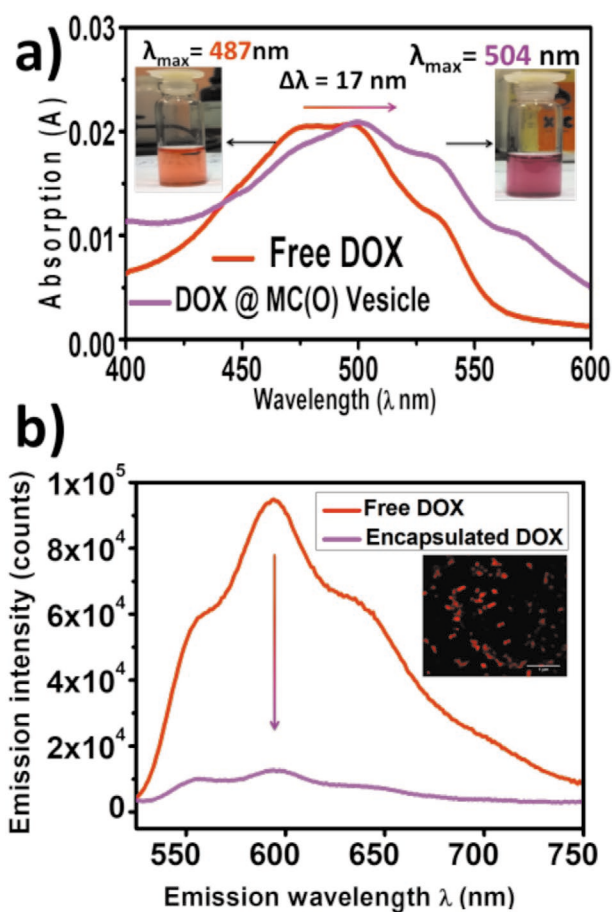


Figure 5. a) UV-vis and b) emission spectra (inset: fluorescence microscope image of DOX encapsulated MC(O) vesicles).

To explore such possibility in vitro, we evaluated the cytotoxicity of free MC(O)-vesicle and DOX@MC(O)-vesicle (prepared and dialyzed in DMSO/water as described in Experimental Section) in various cell lines, namely RAW 264.7 (mouse macrophage), MDA-MB-231 and MCF-7 (both human breast cancer cell lines) in DMEM in different concentration (see Figure S31, Supporting Information); % cell survival and corresponding cell death at a concentration of 0.75×10^{-6} M (IC_{50}) are recorded in Table 1.

It is evident from the data that the cell death values were slightly higher for DOX@MC(O)-vesicle as compared to that of free MC(O)-vesicle suggesting partial release of the drug (DOX) inside the cells. Since concentration dependent DLS data suggested disintegration of vesicular aggregates to smaller particles (see Experimental Section), it was necessary to establish that at a concentration of 0.75×10^{-6} M, MC(O) was still capable of self-assembling to form a vesicular aggregate. Dialyzed solution of MC(O) (200×10^{-6} M) in presence of calcein in DMSO:H₂O (2:98, v/v) was diluted to 0.75×10^{-6} M and dialyzed once again for 72 h (see Experimental Section). DLS ($D_h \approx 91$ nm), emission spectra and fluorescence microscopy revealed the existence of vesicular aggregates even at such a low concentration (see Figures S32 and S33, Supporting Information). In a similar fashion, we prepared DOX@MC(O)-vesicle at a concentration of 0.75×10^{-6} M in DMEM:DMSO (98:2, v/v) (see above); both

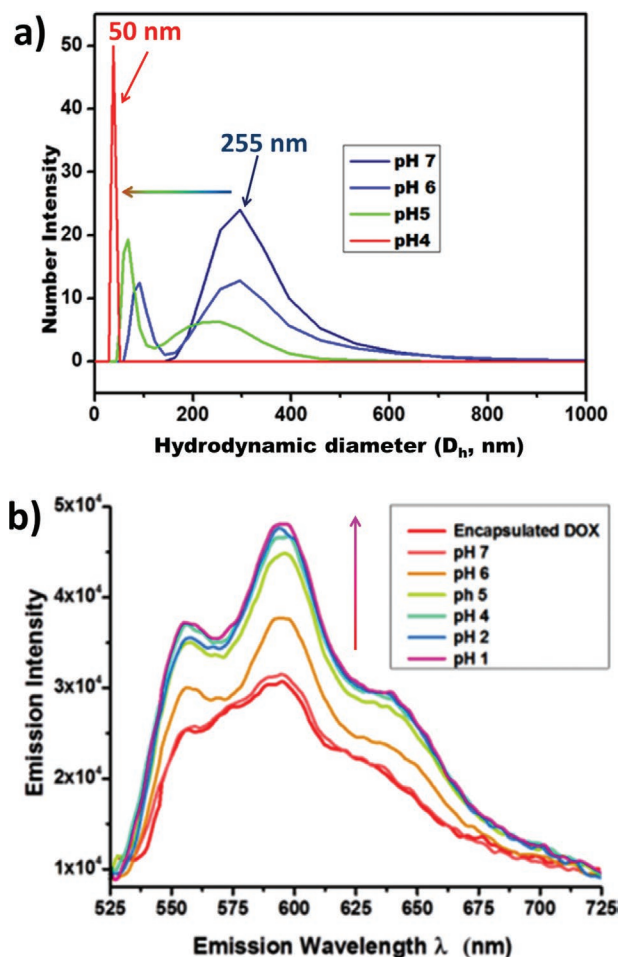


Figure 6. a) pH dependent DLS data of MC(O)-vesicle and b) pH dependent emission spectra ($\lambda_{\text{ex}} = 504$ nm) of DOX@MC(O)-vesicle.

DLS ($D_h \approx 70$ nm) and fluorescence imaging established the existence of vesicles containing DOX (see Figures S34–S36, Supporting Information). With this solution, we performed MTT assay, cell migration and cell imaging studies following literature procedure^[39] in a selected cancer cell line namely MDA-MB-231 (Table 1, Figure S37, Supporting Information); interestingly, the cell death (44%) was comparable to that of DOX@MC(O)-vesicle prepared in DMSO/water. Since DOX release from DOX@MC(O)-vesicle took place around pH 6 (see Experimental Section), the MTT results presumably indicated that intracellular pH of MDA-MB-231 was not conducive enough to

break open the vesicular aggregate to a significant extent. Cell migration assay performed on the same cell line with the same DOX@MC(O)-vesicle (i.e., 0.75×10^{-6} M in DMEM:DMSO, 98:2, v/v) revealed that the cell migration speed ($\approx 12 \mu\text{m h}^{-1}$) in presence of DOX loaded vesicle was marginally slower than that of ($\approx 16 \mu\text{m h}^{-1}$) in control experiment (Figure 7) (i.e., in presence of only DMEM) which corroborated well with that of MTT data (Table 1).

To see how the drug (DOX) is being delivered into the cells, we performed confocal laser scanning microscopy (CLSM) of MDA-MB-231 cells treated with free DOX and DOX@MC(O)-vesicle maintaining the same concentration of free DOX (10.4 nmol L^{-1}) as that available in DOX@MC(O)-vesicle keeping all other conditions identical (Figure 8, see Experimental Section). It was clear from the images that the free DOX as expected was located mostly on the nucleus. On the other hand, images of the DOX@MC(O)-vesicle treated cells displayed localization of DOX mainly in the cytosol with evidence of being able to penetrate into the nucleus albeit to a lesser extent. Thus, all the data (MTT, cell migration and CLSM images) clearly indicated that the drug (DOX) was transported into the cancer cells and slowly delivered to the target site (nucleus) avoiding burst release.

3. Conclusions

The simple M_2L_4 type cationic metallacryptands were reported to form hierarchical self-assembled vesicular structures in various solvent systems including biological media, namely DMEM. Various data (DLS, TEM, AFM, absorption and emission spectra, and fluorescence microscopic images) accumulated on the dilute solution of the MCs in absence and in presence of a highly fluorescent dye (calcein) or drug (DOX) clearly supported the formation of single layered vesicular aggregates. Such self-assembling behavior is consistent with the counterion-mediated charge regulation driven spontaneous self-assembly reported by a handful cationic metal–organic polyhedra. MTT, cell migration assays, and fluorescence confocal microscopy conducted on MDA-MB-231 breast cancer cell line in presence of free and DOX-loaded MC(O)-vesicle confirmed its ability to be transported within the cancer cells. To the best of our knowledge, cationic metallacryptands of the type M_2L_4 displaying such ability to form vesicular aggregates and subsequent ability to load and transport a drug inside cancer cells in biological media are unprecedented. Structural simplicity of the metallacryptands compared to the MOPs reported thus far as vesicle-forming agents offer new opportunities for further functionalization and hence, new properties.

Table 1. MTT data.^{a)}

	RAW 264.7		MDA-MB-231		MCF-7	
	Survival [%]	Death [%]	Survival [%]	Death [%]	Survival [%]	Death [%]
MC(O)-vesicle (DMSO/water)	59 ± 3	41 ± 7	61 ± 6	39 ± 4	59 ± 5	41 ± 5
DOX@MC(O)-vesicle (DMSO/water)	57 ± 4	43 ± 6	52 ± 5	48 ± 5	51 ± 3	49 ± 7
DOX@MC(O)-vesicle (DMSO/DMEM)	–	–	66 ± 4	34 ± 6		

^{a)}All experiments were performed at $IC_{50} = 0.75 \times 10^{-6}$ M with respect to MC(O)-vesicle.

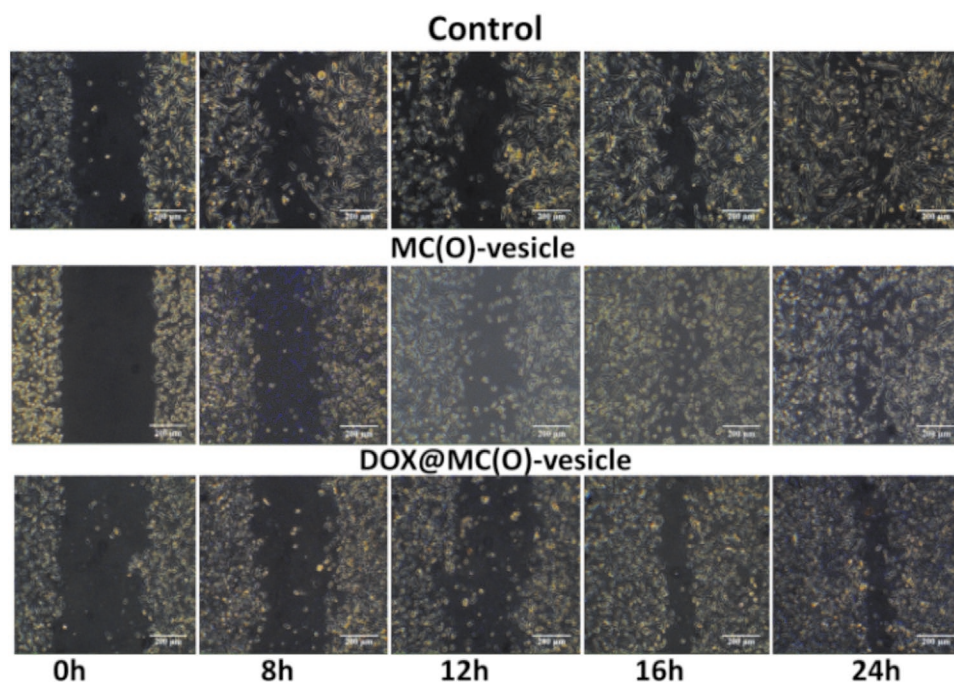


Figure 7. Cell migration assay in MDA-MB-231.

4. Experimental Section

All the chemicals and solvents were commercially available, were purchased and used without further purification. All the ligands (L_x ; X = O, S, C) were synthesized following literature procedure.^[40] ^1H , ^{13}C NMR spectra were recorded using 400 MHz/500 MHz spectrometer (Bruker Ultrashield Plus 400/500). FT-IR spectra were recorded on a FT-IR instrument (FTIR-8300, Shimadzu). Single crystal data were collected in BRUKER APEX II diffractometer equipped with CCD area detector. X-ray powder diffraction data were collected on a Bruker AXS D8 Advance Powder (Cu $K\alpha$ radiation, $\lambda = 1.5406 \text{ \AA}$) X-ray powder diffractometer. TEM images were recorded using a JEOL instrument in the 300 mesh copper TEM grid. TGA analyses were performed on a SDT Q Series 600 Universal VA.2E TA instrument. Diameter measurement of the vesicle from TEM images and processing of cell images were performed using ImageJ software (version 1.41o/java 1.8.0_45). AFM images were taken with an NTMDT instrument, model no. AP-0100 in semi-contact mode. UV-vis spectroscopic measurements were carried out on a Hewlett-Packard 8453 diode array spectrophotometer equipped with a Peltier temperature controller. Emission spectra were recorded with a Horiba Jobin Yvon Fluoromax-4 spectro-fluorimeter. Dynamic light scattering experiments were executed using Malvern Particle Size Analyser (Model No. ZEN 3690 ZETASIZER NANO ZS 90 version 7.03). A METTLER TOLEDO pH meter with microprobe was used to measure the pH of the solutions. Cell images were acquired on an inverted confocal Carl Zeiss microscope. MTT assays were conducted using a multi-plate ELISA reader (Varioskan Flash Elisa Reader, Thermo Fisher).

Synthesis of the Ligand L_C : 3-Aminopyridine (1.0 g, 10 mmol) in dry DCM (150 mL) was taken in a RB (500 mL). To this, dry triethylamine (3 mL) was added dropwise with constant stirring under nitrogen atmosphere. The reaction mixture was cooled in salt-ice bath for 30 min. Solid triphosgene (1.0 g, 3.37 mmol) was added to it and stirred for 45 min keeping the reaction temperature around 0–5 °C. 4,4'-Oxydianiline (1.06 g, 5.3 mmol) dissolved in dry DCM (50 mL) was added dropwise to the reaction mixture under cold condition (0–5 °C). A light pink color was observed. The reaction mixture was stirred for 6 h at room temperature. A light pink-white precipitate was formed. The precipitate was washed with 5% aqueous NaHCO_3 solution (200 mL),

filtered and dried in a desiccator that afforded the pure product as white precipitate. The other two ligands were synthesized by reacting the corresponding dianilines following the same procedure described above.

Lo: ^1H NMR (400 MHz, DMSO-d_6 , 25 °C, δ): 8.87 (s, 1H), 8.83 (s, 1H), 8.58 (s, 1H), 8.17–8.16 (d, $j = 4$, 2H), 7.94–7.91 (d, $j = 12$, 2H), 7.45–7.43 (d, $j = 8$, 2H), 7.31–7.28 (m, 1H), 6.94–6.92 (d, $j = 8$, 2H) ppm (see Figure S1, Supporting Information); ^{13}C NMR (100 MHz, DMSO-d_6 , 25 °C, δ): 152.7, 152.0, 142.8, 140.0, 136.5, 134.8, 125.1, 123.6, 120.2, 118.8 ppm (see Figure S2, Supporting Information); ESI-MS (MeOH): calculated for $[\text{M} + \text{H}]^+$ is 441.41, found 441.17 (Figure S3, Supporting Information). FT-IR: $\bar{\nu} = 3265$ (brs, Urea N–H stretch), 1652 cm^{-1} (s, Urea $>\text{C}=\text{O}$ asymmetric stretch) (see Figure S4, Supporting Information).

Ls: ^1H NMR (400 MHz, DMSO-d_6 , 25 °C, δ): $\delta = 9.26$ (s, 2H), 8.62–8.6 (d, $j = 8$, 1H), 8.17–8.16 (d, $j = 4$, 1H), 7.93–7.91 (d, $j = 8$, 1H), 7.48–7.46 (d, $j = 8$, 2H), 7.30–7.27 (m, 2H), 7.25–7.23 (d, $j = 8$, 2H) (see Figure S5, Supporting Information); ^{13}C NMR (100 MHz, DMSO-d_6 , 25 °C, δ): 152.7, 143.0, 140.2, 138.9, 136.3, 131.7, 127.9, 125.4, 123.6, 119.4, 114.8 ppm (see Figure S6, Supporting Information); MALDI-TOF mass spectroscopy (MeOH-DHB Matrix): Calculated for $[\text{M} + \text{H}]^+$ is 457.52, found 457.411 (see Figure S7, Supporting Information). FT-IR: $\bar{\nu} = 3291$ (brs, Urea N–H stretch), 1637 cm^{-1} (s, Urea $>\text{C}=\text{O}$ asymmetric stretch) (see Figure S8, Supporting Information).

Lc: ^1H NMR (400 MHz, DMSO-d_6 , 25 °C, δ): 8.77 (s, 1H), 8.70 (s, 1H), 8.56 (s, 1H), 8.16–8.15 (d, $j = 4$, 1H), 7.91–7.89 (d, $j = 4$, 1H), 7.35–7.33 (d, $j = 8$, 2H), 7.30–7.27 (m, 1H), 7.12–7.10 (d, $j = 8$, 2H), 3.80 (s, 1H) ppm (see Figure S9, Supporting Information); ^{13}C NMR (100 MHz, DMSO-d_6 , 25 °C, δ): 152.6, 142.8, 140.0, 137.3, 136.5, 135.4, 129.0, 125.2, 123.6, 118.7, 41.2 ppm (see Figure S10, Supporting Information); MALDI-TOF mass spectroscopy (MeOH-DHB Matrix): Calculated for $[\text{M} + \text{H}]^+$ is 439.49, found 439.44 (see Figure S11, Supporting Information). FT-IR: $\bar{\nu} = 3302$ (brs, Urea N–H stretch), 1652 cm^{-1} (s, Urea $>\text{C}=\text{O}$ asymmetric stretch) (see Figure S12, Supporting Information).

Synthesis of the Metallacryptands (MCs): An aqueous solution as a source of CuSiF_6 prepared by taking $\text{Cu}(\text{BF}_4)_2$ (6 mg, 0.025 mmol) and $(\text{NH}_4)_2\text{SiF}_6$ (4 mg, 0.025 mmol) in water (2 mL) was carefully layered over a solution of the corresponding ligand (L_x) prepared by dissolving L_x (0.05 mmol) in DMF (4 mL) and further diluted with EtOH (9 mL) taken in a beaker (25 mL) covered with perforated parafilm at room

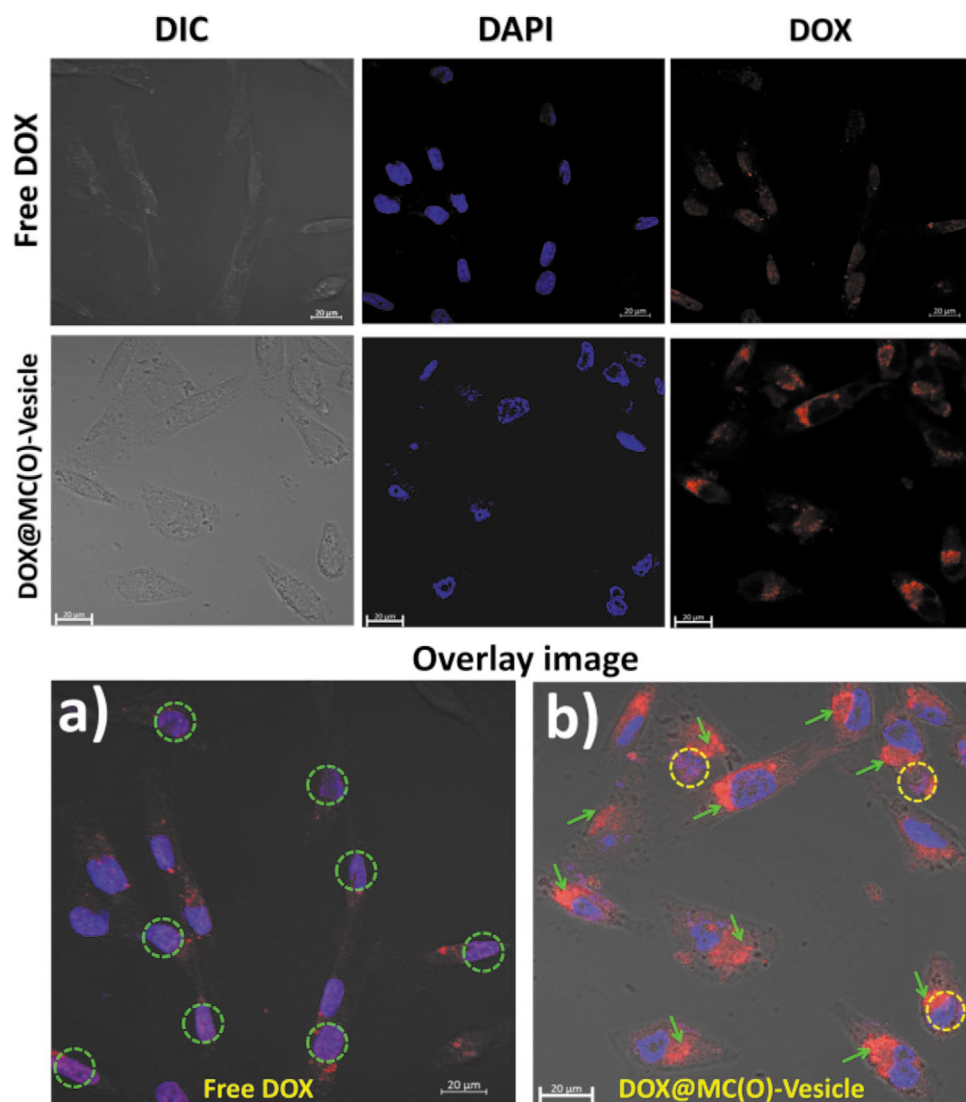


Figure 8. Confocal microscope images of MDA-MB-231 under various conditions. a) Green circles depict localization of DOX in the nucleus. b) Green arrows indicate localization of DOX in the cytosol, yellow circles point out small amount of DOX within the nucleus.

temperature. Block-shaped blue crystals were isolated after 3 weeks, dried in air and used for further characterizations including single crystal X-ray diffraction.

MC(O): Yield (17.8%, 4.62 mg); elemental analysis calcd. (%) for $C_{100}H_{80}Cu_2F_{12}N_{24}O_{14}Si_2 \cdot 17 H_2O$: C 47.71, H 4.80, N 13.35; found: C 47.68, H 4.87, N 13.69; FT-IR: $\bar{\nu} = 3361, 3200, 1706, 1656, 1590, 1552, 1502, 1483, 1432, 1287, 1214, 1070, 1015, 735, 695, 473 \text{ cm}^{-1}$ (see Figure S13, Supporting Information).

MC(S): Yield (19.9%, 5.14 mg, 0.024 mmol); elemental analysis calcd. (%) for $C_{100}H_{80}Cu_2F_{12}N_{24}O_{26}S_4Si_2 \cdot 7H_2O$: 48.91, H 4.35, N 14.69, found: C 48.96, H 4.01, N 14.58; FT-IR: $\bar{\nu} = 3363, 1716, 1655, 1590, 1587, 1552, 1530, 1484, 1433, 1397, 1301, 1280, 1210, 1013, 801, 738, 696, 652, 475 \text{ cm}^{-1}$ (see Figure S14, Supporting Information).

MC(C): Yield: (12.5%, 3.12 mg, 0.012 mmol); elemental analysis calcd. (%) for $C_{104}H_{88}Cu_2F_{12}N_{24}O_{18}Si_2 \cdot 14H_2O$: C 48.73, H 4.37, N 14.11; found: C 48.67, H 4.68, N 14.44; FT-IR: $\bar{\nu} = 3369, 1706, 1590, 1550, 1537, 1484, 1432, 1411, 1296, 1215, 1067, 1022, 801, 738, 697, 475 \text{ cm}^{-1}$ (see Figure S15, Supporting Information).

Single Crystal X-ray Diffraction Study (SXRD): Suitable single crystal was optically chosen, taken in paratone oil, and mounted on a glass fiber. Single crystal X-ray data were collected using MoK_{α} ($\lambda = 0.7107$

\AA) radiation on a SMART APEX-II diffractometer equipped with CCD area detector. Data collection, data reduction, structure solution, and refinement were carried out using the software package of SMART APEX-II. The structure was solved by direct method and refined by full-matrix least-squares based on F^2 values against all reflections in SHELXL-2014^[41] suite of APEX3. Final refinement and CIF finalization were carried out using OLEX2^[42] version 1.2.8. One of the phenyl rings in MC(O) was found to be disordered over two orientations. The disordered model was handled by OLEX2; the site occupancy factors for the disordered atoms of the phenyl ring were refined to 0.504 and 0.496. In all the cases, non-hydrogen atoms were anisotropically refined. The hydrogen atoms were located on calculated positions in the difference Fourier map and refined. Structural simplifications were done for MCs using Topos Pro program.^[43] Crystallographic data for the structural analysis of compounds reported herein have been deposited at the Cambridge Crystallographic Data (CCDC No. 1835283-85).

Powder X-ray Diffraction (PXRD) Study: PXRD data were collected using Bruker AXS D8 Advance Powder (CuK_{α} radiation, $\lambda = 1.5406 \text{ \AA}$) Diffractometer equipped with super speed LYNXEYE detector. The sample was prepared by placing a finely powdered sample ($\approx 20 \text{ mg}$)

over a glass slide. The experiment was carried out with a scan speed of 0.2 s per step (step size = 0.02°) for the scan range of 5–35° (2 θ).

Transmission Electron Microscopy (TEM): Samples for TEM images were prepared by drop casting DMSO solution of MCs (5 μ L, 200 \times 10⁻⁶ M) under study on a carbon-coated Cu grid (300 mesh) followed by drying under vacuum at room temperature for 1 d. TEM images were recorded at an accelerating voltage of 200 kV without any staining.

Atomic Force Microscopy (AFM): DMSO solution (20 μ L, 200 \times 10⁻⁶ M) of the MCs was drop casted on a clean surface of a mica foil (1.0 \times 1.0 cm) glued to an AFM stub and dried under vacuum overnight at room temperature. The AFM images were recorded in semicontact mode; the image and height profile analysis were carried out using WSxM 5.0 Develop software.

Dynamic Light Scattering (DLS) experiment: The solutions of the MCs (1 mL) were taken in a standard DLS glass cuvette (1 \times 1 \times 5 cm) and particle size was measured in a Malvern Particle Size Analyser instrument. All the measurements were done at the scattering angle of 173°. DMSO and milli-Q water were used as a solvent for the measurements.

Calcein Encapsulation within the Vesicles: A solution of calcein (20 μ L in MeOH taken from a stock solution prepared by dissolving 2.2 mg calcein in 10 mL MeOH) was taken in a vial (5 mL) and evaporated to dryness by slow heating; then 1.0 mg of the corresponding MC was added following 40 μ L DMSO. The mixture was further diluted with water (1960 μ L) to make the initial concentration of calcein 3.5 \times 10⁻⁶ M. The resulting solution was then subjected to dialysis (SnakeSkin dialysis tubing, molecular weight cutoff 3500) in a beaker (500 mL) containing 300 mL of water/DMSO (98:2, v/v); the bulk solvent was replaced with the fresh stock of solvent 8 hourly for 72 h. The completion of dialysis was confirmed by the disappearance of characteristic absorption spectra of calcein in the bulk solvent. The concentration and consequently the loading of calcein and its emission spectra in the vesicles were determined by UV–vis and photoluminescence spectroscopy.

Doxorubicin Encapsulation within the MC(O)-vesicle: Doxorubicin: HCl (DOX) (0.1 mg) (100 μ L in MeOH taken from a stock solution prepared by dissolving 1 mg DOX in 1 mL MeOH) was evaporated to dryness by slow heating) was taken in a vial (5 mL); then 1.0 mg of the MC(O) was added following 40 μ L DMSO. The mixture was further diluted with water (1960 μ L) to make the initial concentration of DOX 0.05 mg mL⁻¹. The resulting solution was then subjected to dialysis (SnakeSkin dialysis tubing, molecular weight cutoff 3500) in a beaker (500 mL) containing 300 mL of water/DMSO (98:2, v/v); the bulk solvent was replaced with the fresh stock of solvent 8 hourly for 72 h. The completion of dialysis was confirmed by the disappearance of characteristic absorption spectra of DOX in the bulk solvent. The concentration and consequently the loading of DOX and its emission spectra in the vesicles were determined by UV–vis and photoluminescence spectroscopy.

DLS as a Function pH: DMSO stock solution of MC(O) (2 mL, 200 \times 10⁻⁶ M) was taken in three different vials (5 mL). 1(N) HCl (maximum 20 μ L) was necessary to change the pH of the solutions to 6, 5, and 4 (checked by pH paper). The solutions were kept for 20 min and then subjected to DLS measurements.

Preparation of 0.75 \times 10⁻⁶ M DOX@MC(O)-vesicle in DMEM: DOX (0.1 mg, 100 μ L were taken out from a methanol stock solution of 1 mg mL⁻¹) was taken in a glass vial (5 mL); to it, MC(O) (1 mg) was added; the content of the vial was dissolved in cell culture grade DMSO (2 mL). The resulting solution was then diluted to 0.75 \times 10⁻⁶ M (with respect to MC(O)) with DMEM. The diluted solution was the dialyzed for 72 h as described in above; instead of DMSO/water (2:98, v/v) as described in above, the bulk solution was DMSO/DMEM (2:98, v/v); the dialyzed solution was then subjected to DLS and fluorescence microscopy. All the work like vesicle solution preparation and dialysis experiments were performed in biological hood to avoid possible contaminations.

Stimuli (pH) Responsive Release of DOX from DOX@MC(O)-vesicle: DMSO/water (2:98) stock solution of DOX@MC(O)-vesicle (2 mL, 200 \times 10⁻⁶ M) was taken in a vial (5 mL). Dilute HCl (maximum 30 μ L) was necessary to change the pH of the solutions up to pH 1. With

the change of pH emission intensity of DOX was recorded. The time dependent DOX release experiment was done by setting the pH of the DOX@MC(O)-vesicle at pH 5 with addition of dilute HCl in a pH meter.

MTT assay of MC(O)-vesicle: The cells (RAW 264.7, MDA-MB-231 and MCF7) were grown in high-glucose Dulbecco's modified Eagle's medium (DMEM) supplemented with 10% fetal bovine serum (FBS) and 1% penicillin and streptomycin in a humidified incubator at 37 °C under 5% CO₂ atmosphere. The cells were seeded in a 96-well plate for each experiment at a density of \approx 10⁴ cells per well. After incubation (24 h in humidified incubator at 37 °C under 5% CO₂ atmosphere), various concentrations (up to 1 \times 10⁻⁶ M) of MC(O)-vesicle, DOX@MC(O)-vesicle and DMEM alone (control experiment) were applied to the cells and the mixtures were incubated at 37 °C under 5% CO₂ atmosphere for 72 h. Then the culture medium of each well of the 96-well plate was replaced with the MTT reagent (0.5 mg mL⁻¹, 150 μ L of MTT solution in DMEM) and it was left for 2 h under incubation followed by replacing the media with DMSO (100 mL) to dissolve the formazan produced by the mitochondrial reductase of the live cells. The color intensity of formazan (deep purple), attributed to the live-cell concentration (cell viability), was measured by a multi-plate ELISA reader at 570 nm. The percentage of the cells alive in DOX@MC(O)-vesicle/MC(O)-vesicle was calculated by considering the DMEM-treated sample as control, i.e., 100%. All experiments were performed thrice.

Cell Migration Assay: MDA-MB-231 cells were seeded in 35 mm six-well plate and incubated for 24 h at 37 °C under 5% CO₂ atmosphere to attain maximum confluency. A scratch was introduced in the middle of the plate by the tip of a sterile pipette. Dialyzed DOX@MC(O)-vesicle (1 mL, 0.75 \times 10⁻⁶ M, i.e., the IC₅₀ of free MC(O)) was added to the cells. For the control experiment, only DMEM and MC(O) vesicle (1 mL, 0.75 \times 10⁻⁶ M) was added; then the cells were kept in incubator at 37 °C in a 5% CO₂ atmosphere. Still images were captured under an optical microscope (OLYMPUS CKX31) with different time intervals over 24 h.

Cell Imaging: The working concentration of DOX@MC(O)-vesicle for cell imaging studies was kept at its IC₅₀, i.e., 0.75 \times 10⁻⁶ M. The amount of DOX present in it was calculated to be 10.4 nmol L⁻¹. Therefore, the same concentration of free DOX was employed to perform the control experiments. The MDA-MB-231 cells were seeded in a 35 mm confocal dish and incubated overnight in humidified incubator at 37 °C in a 5% CO₂ atmosphere. After discarding the media (DMEM 10% fetal bovine serum (FBS) and 1% penicillin and streptomycin), the plates were washed with phosphate-buffered saline (PBS; pH 7.4) followed by incubation with 1 mL of free DOX and DOX@MC(O)-vesicle in DMEM at the specified concentration mentioned above for 30 min at 37 °C under 5% CO₂ atmosphere. Then the media was sucked out and the dishes were washed several times with PBS (pH 7.4) to remove the excess free DOX and DOX@MC(O)-vesicle from the culture plate; then the cells were fixed with 4% paraformaldehyde. Finally, the dishes were washed with PBS (pH 7.4) to remove paraformaldehyde followed by treatment with DAPI (0.1 μ g mL⁻¹) in PBS (pH 7.4) for nucleus staining for 10 min; once again the dishes were washed thoroughly with PBS. Finally, PBS (1 mL; pH 7.4) was added to each dish and images were recorded using a Carl Zeiss confocal microscope.

Supporting Information

Supporting Information is available from the Wiley Online Library or from the author.

Acknowledgements

P.B. thanks Indian Association for the Cultivation of Science, Kolkata for a research fellowship. P.D. thanks the Department of Science & Technology, New Delhi for financial support (Grant Nos. EMR/2016/000894 and CRG/2019/000790). The authors thank Professor Narayan Pradhan for TEM image and Gaurav Das, Arpana Singh for helping in cell imaging.

Single-crystal X-ray diffraction data were collected at the Department of Biotechnology (DBT)-funded X-ray diffraction facility under the Centres of Excellence and Innovation in Biotechnology (CEIB) program, IACS, Kolkata.

Conflict of Interest

The authors declare no conflict of interest.

Keywords

anticancer activity, blackberry vesicle, drug delivery, metallacryptand, supramolecular assembly

Received: February 12, 2020

Revised: March 17, 2020

Published online:

-
- [1] T. Kunitake, *Angew. Chem., Int. Ed. Engl.* **1992**, *31*, 709.
 [2] T. Kunitake, Y. Okahata, *J. Am. Chem. Soc.* **1977**, *99*, 3860.
 [3] J. Voskuhl, B. J. Ravoo, *Chem. Soc. Rev.* **2009**, *38*, 495.
 [4] R. Dong, Y. Zhou, X. Zhu, *Acc. Chem. Res.* **2014**, *47*, 2006.
 [5] W. Jiang, Y. Zhou, D. Yan, *Chem. Soc. Rev.* **2015**, *44*, 3874.
 [6] N. Sakai, S. Matile, *Nat. Chem.* **2009**, *1*, 599.
 [7] M. J. Webber, R. Langer, *Chem. Soc. Rev.* **2017**, *46*, 6600.
 [8] F. M. Menger, M. I. Angelova, *Acc. Chem. Res.* **1998**, *31*, 789.
 [9] E. N. Savariar, S. V. Aathimanikandan, S. Thayumanavan, *J. Am. Chem. Soc.* **2006**, *128*, 16224.
 [10] G. Li, S. Zhang, N. Wu, Y. Cheng, J. You, *Adv. Funct. Mater.* **2014**, *24*, 6204.
 [11] C. Li, S. Zhang, J. Pang, Y. Wu, Z. Gu, *Adv. Funct. Mater.* **2015**, *25*, 3764.
 [12] H. T. Baytekin, B. Baytekin, A. Schulz, A. Springer, T. Gross, W. Unger, M. Artamonova, S. Schlecht, D. Lentz, C. A. Schalley, *Chem. Mater.* **2009**, *21*, 2980.
 [13] H. T. Baytekin, B. Baytekin, A. Schulz, C. A. Schalley, *Small* **2009**, *5*, 194.
 [14] N. Giri, S. L. James, *Chem. Commun.* **2011**, *47*, 245.
 [15] N. Giri, S. L. James, *Chem. Commun.* **2011**, *47*, 1458.
 [16] Y. Wei, L. Wang, J. Huang, J. Zhao, Y. Yan, *ACS Appl. Nano Mater.* **2018**, *1*, 1819.
 [17] D. Samanta, S. Roy, R. Sasmal, N. D. Saha, K. R. Pradeep, R. Viswanatha, S. S. Agasti, T. K. Maji, *Angew. Chem., Int. Ed.* **2019**, *58*, 5008.
 [18] K. Sarkar, M. Paul, P. Dastidar, *Chem. Commun.* **2016**, *52*, 13124.
 [19] T. Liu, *J. Am. Chem. Soc.* **2003**, *125*, 312.
 [20] D. Li, J. Zhang, K. Landskron, T. Liu, *J. Am. Chem. Soc.* **2008**, *130*, 4226.
 [21] D. Li, W. Zhou, K. Landskron, S. Sato, C. J. Kiely, M. Fujita, T. Liu, *Angew. Chem.* **2011**, *123*, 5288.
 [22] A. A. Verhoeff, M. L. Kistler, A. Bhatt, J. Pigga, J. Groenewold, M. Klokkenburg, S. Veen, S. Roy, T. Liu, *Phys. Rev. Lett.* **2007**, *99*, 066104.
 [23] M. Paul, N. N. Adarsh, P. Dastidar, *Cryst. Growth Des.* **2014**, *14*, 1331.
 [24] J. M. Lehn, *Angew. Chem., Int. Ed. Engl.* **1988**, *27*, 89.
 [25] C. A. Ilioudis, D. A. Tocher, J. W. Steed, *J. Am. Chem. Soc.* **2004**, *126*, 12395.
 [26] P. Ghosh, S. Sengupta, P. K. Bharadwaj, *Langmuir* **1998**, *14*, 5712.
 [27] N. N. Adarsh, D. A. Tocher, J. Ribasc, P. Dastidar, *New J. Chem.* **2010**, *34*, 2458.
 [28] T. Liu, E. Diemann, H. Li, A. W. M. Dress, A. Muller, *Nature* **2003**, *426*, 59.
 [29] G. Liu, Y. Cai, T. Liu, *J. Am. Chem. Soc.* **2004**, *126*, 16690.
 [30] G. Liu, T. Liu, *J. Am. Chem. Soc.* **2005**, *127*, 6942.
 [31] M. L. Kistler, A. Bhatt, G. Liu, D. Casa, T. Liu, *J. Am. Chem. Soc.* **2007**, *129*, 6453.
 [32] L. E. Euliss, J. A. DuPont, S. Gratton, J. DeSimone, *Chem. Soc. Rev.* **2006**, *35*, 1095.
 [33] J. Boucard, C. Linot, T. Blondy, S. Nedellec, P. Hulin, C. Blanquart, L. Lartigue, E. Ishow, *Small* **2018**, *14*, 1802307.
 [34] S. Jia, W. K. Fong, B. Graham, B. J. Boyd, *Chem. Mater.* **2018**, *30*, 2873.
 [35] J. H. Lee, H. Oh, U. Baxa, S. R. Raghavan, R. Blumenthal, *Biomacromolecules* **2012**, *13*, 3388.
 [36] R. Ghaffarian, E. Perez-Herrero, H. Oh, S. R. Raghavan, S. Muro, *Adv. Funct. Mater.* **2016**, *26*, 3382.
 [37] J. R. Griffiths, *Br. J. Cancer* **1991**, *64*, 425.
 [38] R. A. Gatenby, R. J. Gillies, *Nat. Rev. Cancer* **2004**, *4*, 891.
 [39] J. Deb, J. Majumder, S. Bhattacharyya, S. S. Jana, *BMC Cancer* **2014**, *14*, 567.
 [40] D. B. Grotjahn, C. Joubran, *Tetrahedron: Asymmetry* **1995**, *6*, 745.
 [41] G. M. Sheldrick, *Acta Crystallogr., Sect. A: Found. Adv.* **2015**, *71*, 3.
 [42] O. V. Dolomanov, L. J. Bourhis, R. J. Gildea, J. A. K. Howard, H. Puschmann, *J. Appl. Crystallogr.* **2009**, *42*, 339.
 [43] V. A. Blatov, A. P. Shevchenko, D. M. Proserpio, *Cryst. Growth Des.* **2014**, *14*, 3576.